# Design of Condensed Molecular Structures for MR-TADF with High Efficiency and Good Color Purity in Deep-Blue Region

*Junyoung Moon[1], Seungwon Han[2], Jun Yeob Lee[1, 2*]*

[1]School of Chemical Engineering, Sungkyunkwan University, 2066, Seobu-ro, Jangan-gu, Suwon-si, Gyeonggi-do, 16419, Republic of Korea

[2]Department of Display Convergence Engineering, Sungkyunkwan University, 2066, Seobu-ro, Jangan-gu, Suwon-si, Gyeonggi-do, 16419, Republic of Korea

[1]Telephone: +82-31-299-4807, E-mail: leej17@skku.edu

## Abstract

***Recent advancements in blue OLED materials have focused on achieving both high efficiency and excellent color purity. Generally, narrow full width at half maximum is essential for excellent color purity, which can be achieved using multi-resonance thermally activated delayed fluorescence (MR-TADF) materials. Here, we report hybrid MR-TADF materials combining boron-based MR-TADF known for high efficiency, and ICz-based MR-TADF, renowned for excellent color purity.***

## Keywords

Keywords: OLEDs; Multi-resonance thermally activated delayed fluorescence; Boron-ICz condensation; Deep-blue emission.

## 1. Objective and Background

Fluorescent organic light-emitting diodes (OLEDs) materials are limited by their inability to utilize triplet excitons for light emission, resulting in an internal quantum efficiency capped at 25%, as only singlet excitons, which constitute 25% of the total excitons, contribute to luminescence. (1–3) Due to the low internal quantum efficiency (IQE), fluorescent materials typically achieve a maximum external quantum efficiency (EQE) of around 5–10%, significantly lower than their phosphorescent or thermally activated delayed fluorescence (TADF) counterparts, which can fully harness both singlet and triplet excitons. (4) Although fluorescent materials offer the advantage of high operational stability and are currently utilized as blue emitting layers in commercial applications, their inherent IQE limitations necessitate continued exploration and development of phosphorescent and TADF materials by researchers.

TADF leverages a mechanism that thermally converts triplet states into singlet states to achieve an IQE of 100%. (4, 5) This process, known as reverse intersystem crossing (RISC), becomes efficient when the energy gap between the triplet and singlet states ($\Delta E_{ST}$) is sufficiently small. To facilitate charge transfer (CT) emission and suppress undesired local emission caused by electron-hole recombination, spatial separation of electron density between the donor and acceptor moieties within the molecule is essential. In contrast to conventional donor-acceptor-based TADF materials, multi-resonance (MR)-TADF emitters are designed with a structure where the electron density of the molecule is localized at specific atoms or groups through resonance effects. (6–9) MR-TADF emitters typically exhibit a much narrower full width at half maximum (FWHM) of 20–40 nm compared to conventional TADF, enabling excellent color purity while suppressing high-energy emissions in the deep-blue region. In 2016, MR-TADF emitters based on boron and nitrogen atoms was developed by Prof. Hatakeyama's lab. (6) It demonstrated excellent emission performance, a narrow FWHM, and TADF characteristics. However, achieving spectra in the deep-blue region remained challenging. In 2021, indolocarbazole (ICz)-based MR-TADF materials were developed by our group, demonstrating narrow FWHM and emission in the short-wavelength region due to its rigid molecular structure. (8) However, the broadened $\Delta E_{ST}$ resulted in weaker TADF characteristics compared to boron-based MR-TADF, leading to a slower RISC rate as a drawback. To overcome the respective limitations of these two types of MR-TADF compounds while integrating their advantages, a hybrid design strategy was adopted. Previously reported hybrid MR-TADF materials with ICz fused at the center of boron-nitrogen-based MR-TADF structures demonstrated enhanced emission efficiency and improved TADF characteristics but exhibited spectra unsuitable for applications in the deep-blue region.(10–13)

In this study, newly designed hybrid MR-TADF materials developed by modifying the position of ICz condensation, demonstrated excellent emission efficiency and TADF characteristics while achieving spectra in the deep-blue region. A t-butyl carbazole group was introduced on the boron-centered donating part, while a substituent with di-t-butyl-indolo[3,2,1-jk]carbazole fused to phenol was used on the opposite donating part. Two new MR-TADF materials were synthesized based on the direction of conjugation and were named BN-OICz and BN-o-OICz. Each of the two materials exhibited emission in the deep-blue region with electroluminescence (EL) peaks at 454 nm and 456 nm and FWHM of 24.5 nm and 25.4 nm in the fabricated devices. They also demonstrated a high maximum EQE ($EQE_{max}$) of 28.7% and 31.0%, respectively.

## 2. Results

The two hybrid MR-TADF materials were obtained through nucleophilic substitution, demethylation, palladium-catalyzed cross-coupling reactions, and boron cyclization. The synthesized materials were confirmed using nuclear magnetic resonance and mass spectroscopy analyses. To predict the optical properties and frontier molecular orbital (FMO) electron distributions of the two molecules, density functional theory (DFT) and time-dependent DFT calculations were performed using the B3LYP/6-31G basis set. The results are presented in **Table 1**.


ISSN 0097-996X/25/5603-2275-$1.00 © 2025

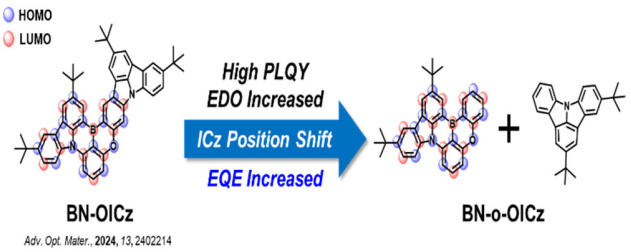


**Figure 1.** Design strategy of hybrid MR-TADF materials.

Highest occupied molecular orbital (HOMO) and lowest unoccupied molecular orbital (LUMO) were extracted from the FMO distribution, and **Figure 1** shows that both materials form multi-resonance structures with electron density localized around the boron-centered atoms and their substituent groups. The formation of MR suggests the potential for TADF implementation. Notably, BN-o-OICz exhibits the planarity extending further into the ICz unit, including its substituent groups, implying that this material is structurally influenced by a slightly broader range of optical effects.

**Table 1.** DFT calculation data of hybrid MR-TADF materials.

| | BN-OICz | BN-o-OICz |
|---|---|---|
| HOMO (eV) | −5.17 | −5.15 |
| LUMO (eV) | −1.65 | −1.67 |
| HOMO–LUMO gap (eV) | 3.52 | 3.48 |
| Oscillator strength (f) | 0.4658 | 0.6113 |

As shown in **Table 1**, despite the differences in HOMO and LUMO electron distributions between the two materials, their energy levels did not exhibit significant differences. The HOMO energy levels were calculated to be −5.17 eV for BN-OICz and −5.15 eV for BN-o-OICz, while the LUMO energy levels were −1.65 eV and −1.67 eV, respectively. The HOMO–LUMO band gaps were determined to be 3.52 eV and 3.48 eV, indicating potential absorption in the blue region. Furthermore, the oscillator strength was calculated as 0.4658 for BN-OICz and 0.6113 for BN-o-OICz, showing high values. These findings suggest that both materials exhibit strong absorption and emission properties, making them promising candidates for OLED applications.

To analyze the photophysical properties of the hybrid MR-TADF materials, UV-visible absorption and photoluminescence (PL) emission spectra were measured at room temperature in THF at a concentration of $10^{-5}$M. Phosphorescence measurements were conducted under 77 K conditions. The results are summarized in **Table 2**.

The absorption peaks of BN-OICz and BN-o-OICz were observed at 435 nm and 437 nm, respectively, with both materials showing strong short range CT characteristics. BN-OICz exhibited slightly stronger absorption in the 300–400 nm range, which can be attributed to the local excitation characteristics influenced by the overlap of HOMO and LUMO at the ICz-fused region. The fluorescence emission properties of both materials at room temperature were nearly identical, with a PL peak ($\lambda_{PL}$) at 450 nm. The FWHM of BN-o-OICz was measured at 24.3 nm, 0.2 nm broader than that of BN-OICz. This slight increase in FWHM is likely due to the planar structure of BN-o-OICz, which does not completely suppress intermolecular interactions.

**Table 2.** Photophysical Characteristics of hybrid MR-TADF materials in THF solution ($10^{-5}$ M).

| Materials | BN-OICz | BN-o-OICz |
|---|---|---|
| $\lambda_{abs}$ (nm) | 435 | 437 |
| $\lambda_{PL}$ (nm) | 450 | 450 |
| FWHM (nm) | 24.1 | 24.3 |
| $E_{S1}$ (eV) | 2.87 | 2.89 |
| $E_{T1}$ (eV) | 2.70 | 2.74 |
| $\Delta E_{ST}$ (eV) | 0.17 | 0.15 |

The singlet excited state energy ($E_{S1}$) was determined from fluorescence emission data and BN-OICz and BN-o-OICz exhibited $E_{S1}$ = 2.87 eV and $E_{S1}$ = 2.89 eV, respectively. Also, the triplet excited state energy ($E_{T1}$) was derived from phosphorescence data, showing $E_{T1}$ = 2.70 eV for BN-OICz and $E_{T1}$ = 2.74 eV for BN-o-OICz. To investigate the TADF characteristics, $\Delta E_{ST}$ was calculated, yielding values of 0.17 eV for BN-OICz and 0.15 eV for BN-o-OICz. These sufficiently small $\Delta E_{ST}$ values indicate the potential for TADF characteristics.

To evaluate the emission efficiency of the two materials, photoluminescence quantum yield (PLQY) measurements were conducted on films prepared by doping 3% of the hybrid MR-TADF materials into 3,3′-di(9H-carbazol-9-yl)-1,1′-biphenyl:diphenyl[4-(triphenylsilyl)-phenyl]phosphine oxide (mCBP:TSPO1) mixed host system. Both materials exhibited high PLQY of 99%, suggesting their potential to achieve high EQE values in device fabrication. The characteristics of the two materials in the film state, including PLQY analysis, are summarized in **Table 3**.

PL spectrum analysis was conducted in the film state. The $\lambda_{PL}$ of BN-OICz and BN-o-OICz were measured at 457 nm and 460 nm, respectively. Unlike the solution PL, where both materials showed identical values, BN-o-OICz exhibited a 3 nm red-shift in the film state. Additionally, the FWHM was measured as 31.4 nm for BN-OICz and 36.3 nm for BN-o-OICz. These results suggest that the planar structure of BN-o-OICz is more susceptible to intermolecular interactions.

Transient PL analysis was performed to examine the radiative rate constants of both materials in the film state. Both materials demonstrated rapid prompt emission with radiative rate constants in the order of $10^8$ $s^{-1}$. The RISC rate constants were measured as $2.04 \times 10^4$ $s^{-1}$ for BN-OICz and $2.46 \times 10^4$ $s^{-1}$ for BN-o-OICz, indicating that BN-o-OICz exhibits a faster RISC rate. Based on these findings, BN-o-OICz is expected to exhibit slightly improved roll-off characteristics.

**Table 3.** Photophysical Characteristics of hybrid MR-TADF materials in film.

| Materials | BN-OICz | BN-o-OICz |
|---|---|---|
| PLQY[(a)] (%) | 99 | 99 |
| $\lambda_{PL}$[(a)] (nm) | 457 | 460 |
| FWHM[(a)] (nm) | 31.4 | 36.3 |
| $k_p$[(a)] ($10^8$ $s^{-1}$) | 1.81 | 1.96 |
| $k_{RISC}$[(a)] ($10^4$ $s^{-1}$) | 2.04 | 2.46 |

(a)3% doped with in mCBP:TSPO1.

To confirm the performance of the two hybrid MR-TADF materials as deep-blue emitters, EL devices were fabricated as illustrated in **Figure 2**.

| |
|---|
| **LiF/Al(1.5/+200)** |
| **TSPO1(25)** |
| **mCBP:TSPO1:hybrid MR-TADF (25:50%:1 wt%)** |
| **mCP(5)** |
| **TCTA(5)** |
| **TAPC(10)** |
| **PEDTO:PSS(40)** |
| **ITO(50)** |

**Figure 2.** Device sturcture of hybrid MR-TADF OLEDs.

Indium tin oxide (ITO, 50 nm) was used as the substrate. Poly(3,4-ethylenedioxythiophene):poly(styrene sulfonate) (PEDOT:PSS, 40 nm) was coated onto the ITO substrate, followed by the deposition of 4,4'-cyclohexylidenebis[N,N-bis(4-methylphenyl)aniline] (TAPC, 10 nm) and Tris(4-carbazoyl-9-ylphenyl)amine (TCTA, 5 nm) as hole transport layers. Subsequently, 1,3-bis(N-carbazolyl)benzene (mCP, 5 nm) was introduced as the electron blocking layer, while the emissive layer (EML) consisted of a mixed host and dopant system with mCBP:TSPO1:hybrid MR-TADF (25 nm:50%:1 wt%). This was followed by tris(4-carbazoyl-9-ylphenyl)amine (TSPO1, 25 nm) as the electron transport layer, LiF (1.5 nm) as the electron injection layer, and Al (200 nm) as the cathode. The properties of the fabricated devices are summarized in **Figure 3** and **Table 4**.

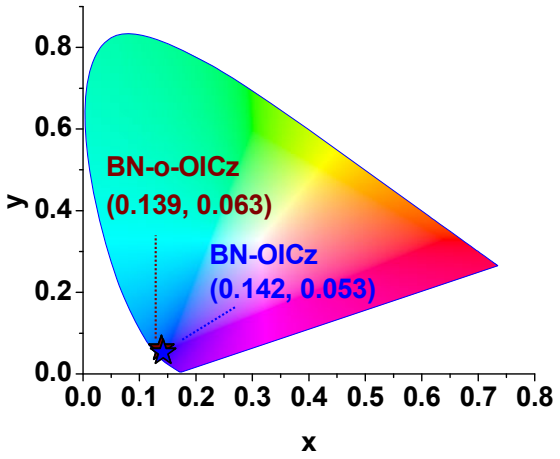


**Figure 3.** CIE coordinates of hybrid MR-TADF devices.

The device based on BN-OICz operated at 4.3 V, while the BN-o-OICz-based device operated at a slightly lower voltage of 4.1 V. Both devices exhibited deep-blue emission, with BN-OICz showing an EL peak ($\lambda_{EL}$) at 454 nm and a FWHM of 24.5 nm, and BN-o-OICz showing an $\lambda_{EL}$ at 456 nm and a FWHM of 25.4 nm. As mentioned earlier, the slightly broader FWHM of BN-o-OICz is attributed to its planar molecular structure. As a result, BN-OICz achieved the $EQE_{max}$ of 28.7% at CIE coordinates (0.142, 0.053), while BN-o-OICz exhibited the $EQE_{max}$ of 31.0% at CIE coordinates (0.139, 0.063), demonstrating superior emission efficiency. At a luminance of 100 cd $m^{-2}$ , BN-o-OICz exhibited the roll-off of 38%, which is slightly improved compared to the 45% roll-off of BN-OICz. This result can be attributed to the smaller $\Delta E_{ST}$ of BN-o-OICz. The $EQE_{max}$ of over 30% for BN-o-OICz is derived from its high PLQY of 99% and planar molecular structure. The planar structure contributes to an enhanced emitting dipole orientation (EDO), with BN-o-OICz showing the EDO of 87.5% when 3% doped in the mCBP:TSPO1 mixed host. In comparison, BN-OICz, which achieved the $EQE_{max}$ of 28.7%, exhibited the slightly lower EDO of 85.0%.

**Table 4.** Device performance of hybrid MR-TADF materials (1 wt% doped).

| | BN-OICz | BN-o-OICz |
|---|---|---|
| $V_d$[(a)] (V) | 4.3 | 4.1 |
| $EQE_{max}$ (%) | 28.7 | 31.0 |
| $EQE_{100}$ (%) | 15.7 | 19.3 |
| $\lambda_{EL}$ (nm) | 454 | 456 |
| FWHM (nm) | 24.5 | 25.4 |
| CIE (x, y) | (0.142, 0.053) | (0.139, 0.063) |

(a) Values at 100 cd $m^{-2}$ .

## 3. Impact of Research

The significance of this study lies in showcasing the potential of

hybrid MR-TADF materials, designed by condensing boron-based MR-TADF and ICz-based MR-TADF, for deep-blue TADF emitters. By effectively combining the advantages of both types of MR-TADF, the hybrid materials achieved the high PLQY of 99% and exhibited suitable PL spectra in the deep-blue region. When fabricated as devices using each material as a dopant, BN-OICz and BN-o-OICz exhibited deep-blue emission with $CIE_y$ values of 0.053 and 0.063, respectively, which are close to the BT.2020 blue standard CIEy value of 0.046. Notably, BN-o-OICz exhibited a high efficiency with the $EQE_{max}$ of 31.0%. Further strucutral modifications are anticipated to achieve the materials to achieve color purity suitable for BT.2020 blue standard while maintaining high efficiency.

## 4. References

1. Bai K, Li M, Tan X, Dai L, Liang K, Li H, et al. Reducing intersystem crossing rates of boron emitters for high-efficiency and long-lifetime deep-blue OLEDs. Journal of Materials Chemistry C. 2023;11(46):16159-67.
2. Cheng C, Zhu Y, Tsuboi T, Deng C, Lou W, Liu T, et al. Extremely stable deep-blue organic light-emitting diodes employing diindolophenazine-based fluorophore with narrow-band emission and a shallow LUMO level. Chemical Engineering Journal. 2023;474.
3. Kang J, Lee HL, Jeon SO, Bae HJ, Kim SC, Han S, et al. Spin-Flip-Restricted Multiple-Resonance Emitters for Extended Device Lifetime in Indolocarbazole-Based Blue Organic Light-Emitting Diodes. Advanced Science. 2024;11(40):e2405604.
4. Uoyama H, Goushi K, Shizu K, Nomura H, Adachi C. Highly efficient organic light-emitting diodes from delayed fluorescence. Nature. 2012;492(7428):234-8.
5. Zhang Q, Li B, Huang S, Nomura H, Tanaka H, Adachi C. Efficient blue organic light-emitting diodes employing thermally activated delayed fluorescence. Nature Photonics. 2014;8(4):326-32.
6. Hatakeyama T, Shiren K, Nakajima K, Nomura S, Nakatsuka S, Kinoshita K, et al. Ultrapure Blue Thermally Activated Delayed Fluorescence Molecules: Efficient HOMO-LUMO Separation by the Multiple Resonance Effect. Advanced Materials. 2016;28(14):2777-81.
7. Mamada M, Hayakawa M, Ochi J, Hatakeyama T. Organoboron-based multiple-resonance emitters: synthesis, structure-property correlations, and prospects. Chemical Society Reviews. 2024;53(3):1624-92.
8. Patil VV, Lee HL, Kim I, Lee KH, Chung WJ, Kim J, et al. Purely Spin-Vibronic Coupling Assisted Triplet to Singlet Up-Conversion for Real Deep Blue Organic Light-Emitting Diodes with Over 20% Efficiency and y Color Coordinate of 0.05. Advanced Science . 2021;8(20):e2101137.
9. Patil VV, Hong WP, Lee JY. Indolocarbazole Derivatives for Highly Efficient Organic Light-Emitting Diodes. Advanced Energy Materials. 2024.
10. Luo XF, Song SQ, Ni HX, Ma H, Yang D, Ma D, et al. Multiple-Resonance-Induced Thermally Activated Delayed Fluorescence Materials Based on Indolo[3,2,1-jk]carbazole with an Efficient Narrowband Pure-Green Electroluminescence. Angewandte Chemie International Edition. 2022;61(41):e202209984.
11. Luo XF, Ni HX, Shen L, Wang L, Xiao X, Zheng YX. An indolo[3,2,1-jk]carbazole-fused multiple resonance-induced thermally activated delayed fluorescence emitter for an efficient narrowband OLED. Chemical Communication. 2023;59(17):2489-92.
12. Wu ZG, Xin Y, Lu C, Huang W, Xu H, Liang X, et al. Precise Regulation of Multiple Resonance Distribution Regions of a B,N-Embedded Polycyclic Aromatic Hydrocarbon to Customize Its BT2020 Green Emission. Angewandte Chemie International Edition. 2024;63(7):e202318742.
13. He X, Lou J, Li B, Dong X, Zhong F, Liu W, et al. Rational Medium-Range Charge Transfer Strategy Toward Highly Efficient Violet-Blue Organic Light-Emitting Diodes with Narrowed Emission. Advanced Materials. 2024;36(2):e2310417.